University of Nebraska - Lincoln
DigitalCommons@University of Nebraska - Lincoln

Xiaoshan Xu Papers | Research Papers in Physics and Astronomy

2008

Optical band gap of BiFeO3 grown by molecular-beam epitaxy

J. F. Ihlefeld
Pennsylvania State University

N. J. Podraza
Pennsylvania State University

Z. K. Liu
Pennsylvania State University

R. C. Rai
University of Tennessee

X. Xu
University of Nebraska-Lincoln, xiaoshan.xu@unl.edu

See next page for additional authors

Follow this and additional works at: https://digitalcommons.unl.edu/physicsxu

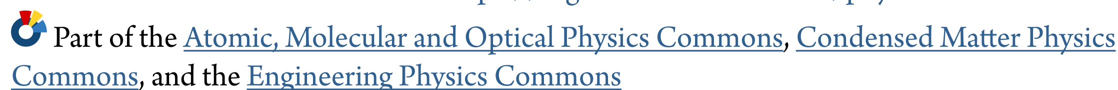
Part of the Atomic, Molecular and Optical Physics Commons, Condensed Matter Physics Commons, and the Engineering Physics Commons

Ihlefeld, J. F.; Podraza, N. J.; Liu, Z. K.; Rai, R. C.; Xu, X.; Heeg, T.; Chen, Y. B.; Li, J.; Collins, R. W.; Musfeldt, J. L.; Pan, X. Q.; Schubert, J.; Ramesh, R.; and Schlom, D. G., "Optical band gap of BiFeO3 grown by molecular-beam epitaxy" (2008). *Xiaoshan Xu Papers*. 29.
https://digitalcommons.unl.edu/physicsxu/29

This Article is brought to you for free and open access by the Research Papers in Physics and Astronomy at DigitalCommons@University of Nebraska - Lincoln. It has been accepted for inclusion in Xiaoshan Xu Papers by an authorized administrator of DigitalCommons@University of Nebraska - Lincoln.

Authors
J. F. Ihlefeld, N. J. Podraza, Z. K. Liu, R. C. Rai, X. Xu, T. Heeg, Y. B. Chen, J. Li, R. W. Collins, J. L. Musfeldt, X. Q. Pan, J. Schubert, R. Ramesh, and D. G. Schlom

This article is available at DigitalCommons@University of Nebraska - Lincoln: https://digitalcommons.unl.edu/physicsxu/29

Optical band gap of $BiFeO_3$ grown by molecular-beam epitaxy

J. F. Ihlefeld,[1,2] N. J. Podraza,[1] Z. K. Liu,[1] R. C. Rai,[3] X. Xu,[3] T. Heeg,[4] Y. B. Chen,[5] J. Li,[6] R. W. Collins,[6] J. L. Musfeldt,[3] X. Q. Pan,[5] J. Schubert,[4] R. Ramesh,[2,7] and D. G. Schlom[1,a)]

[1]*Materials Research Institute, Pennsylvania State University, University Park, Pennsylvania 16802, USA*
[2]*Department of Materials Science and Engineering, University of California, Berkeley, California 94720, USA*
[3]*Department of Chemistry, University of Tennessee, Knoxville, Tennessee 37996, USA*
[4]*Institute for Bio- and Nano-Systems (IBN1-IT), Research Centre Jülich, D-52425 Jülich, Germany*
[5]*Department of Materials Science and Engineering, University of Michigan, Ann Arbor, Michigan 48019, USA*
[6]*Department of Physics and Astronomy, University of Toledo, Toledo, Ohio 43606, USA*
[7]*Department of Physics, University of California, Berkeley, California 94720, USA*

(Received 2 January 2008; accepted 19 February 2008; published online 10 April 2008)

$BiFeO_3$ thin films have been deposited on (001) $SrTiO_3$ substrates by adsorption-controlled reactive molecular-beam epitaxy. For a given bismuth overpressure and oxygen activity, single-phase $BiFeO_3$ films can be grown over a range of deposition temperatures in accordance with thermodynamic calculations. Four-circle x-ray diffraction reveals phase-pure, epitaxial films with ω rocking curve full width at half maximum values as narrow as 29 arc sec (0.008°). Multiple-angle spectroscopic ellipsometry reveals a direct optical band gap at 2.74 eV for stoichiometric as well as 5% bismuth-deficient single-phase $BiFeO_3$ films. © *2008 American Institute of Physics*. [DOI: 10.1063/1.2901160]

$BiFeO_3$ is the only known material that is both ferroelectric ($T_C \sim 1083$ K) and antiferromagnetic ($T_N \sim 625$ K) at room temperature.[1] Recent reports of a large spontaneous polarization ($\sim 100\ \mu C/cm^2$) in thin films,[2] bulk ceramic,[3] and single crystals[4] of $BiFeO_3$ have led to an explosion of interest in its growth and properties.

The ferroelectric and multiferroic properties of $BiFeO_3$ are of interest for a number of applications including devices that utilize heterojunction effects where knowledge of the $BiFeO_3$ band gap is crucial for device design. To date, there is limited and conflicting information on the band gap and optical properties of $BiFeO_3$, with existing reports limited to polycrystalline films[5–7] or nanowires.[8]

We have previously reported the deposition of $BiFeO_3$ films via adsorption-controlled reactive molecular-beam epitaxy (MBE) on (111) $SrTiO_3$ substrates.[9] In this letter, we report the adsorption-controlled growth of $BiFeO_3$ on (001)-oriented $SrTiO_3$ and the resulting crystalline quality, microstructure, optical dielectric functions, and band gap.

Single-crystalline, TiO_2-terminated[10] $SrTiO_3$ substrates aligned within ±0.5° of (001) were used as substrates. Films were grown under conditions described previously.

The parameter space for the adsorption-controlled growth of $BiFeO_3$ was calculated through the CALPHAD method[11] and was empirically established using *in situ* reflection high-energy electron diffraction (RHEED) and confirmed by *ex situ* four-circle x-ray diffraction (XRD). Figure 1 shows a calculated Ellingham diagram representing the phase stability regions of (I) $BiFeO_3 + \gamma\text{-}Fe_2O_3$, (II) $BiFeO_3$, and (III) $BiFeO_3 + Bi_2O_{2.5}$ as a function of substrate temperature and O_2 overpressure. Analogous phase stability diagrams have been calculated from thermodynamic data for the adsorption-controlled growth of III-V compounds,[12–15] MgB_2,[16] $PbTiO_3$,[17] and $Bi_4Ti_3O_{12}$.[12] In the case of $BiFeO_3$ and $Bi_2O_{2.5}$, the Gibbs energies of formation have not been reported. The boundaries between regions I, II, and III were calculated with the Gibbs energy functions of the gas phase containing various Bi and Bi–O species and the stable and metastable iron and bismuth oxides, all taken from the SGTE database.[18] We consider two scenarios for $Bi_2O_{2.5}$ and $BiFeO_3$. The enthalpy of formation of $Bi_2O_{2.5}$ is assumed to be +100 or +4500 J/mol of $Bi_2O_{2.5}$ with respect to the $Bi-Bi_2O_3$ tie line. The enthalpy of formation of $BiFeO_3$ is assumed to be −1000 or −5000 J/mol with respect to the $Bi_2O_3-Fe_2O_3$ tie line. The phase stability region was calculated using THERMOCALC (Ref. 19) with the partial pressure of bismuth fixed at 6.7×10^{-10} atm, which corresponds to the pressure at the plane of the substrate for an incident bismuth flux of 1.4×10^{14} Bi/cm^2 s.[20] The solid lines in Fig. 1 bound

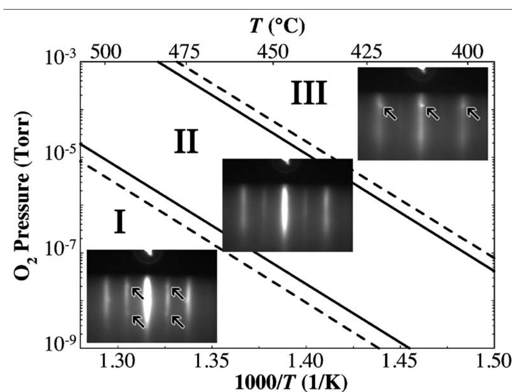

FIG. 1. Calculated Ellingham diagram and RHEED patterns collected along the ⟨110⟩ azimuth of $SrTiO_3$ during Bi–Fe–O deposition at different temperatures and Bi_xO_y gas overpressures. Solid lines represent phase boundaries using +100 and −1000 J/mol formula unit free energies for $Bi_2O_{2.5}$ and $BiFeO_3$, respectively, specifying the narrowest growth window possible, and dashed lines for +4500 and −5000 J/mol formula unit, indicating the approximate uncertainty in width of the growth window. Phase stability between Bi_xO_y gases and $BiFeO_3 + \gamma\text{-}Fe_2O_3$, $BiFeO_3$, and $BiFeO_3 + Bi_2O_{2.5}$ condensed phases is represented by Regions I, II, and III, respectively.

a)Electronic mail: schlom@ems.psu.edu.

 © 2008 American Institute of Physics

the $BiFeO_3$ region with formation enthalpies of +100 and −1000 J/mol for $Bi_2O_{2.5}$ and $BiFeO_3$, respectively, specifying the narrowest growth window possible, while the dashed lines represent the stability for +4500 and −5000 J/mol, indicating the approximate uncertainty in the growth window due to the lack of relevant free energy data.

The thermodynamic predictions were verified by investigating a horizontal slice through this diagram at constant bismuth (Bi flux$=1.4\times10^{14}$ Bi/cm^2 s) and oxygen (O_2+$\sim$10% O_3 background pressure$=1\times10^{-6}$ Torr) overpressure during the deposition of Bi–Fe–O over a temperature range of 375–475 °C and a fixed Bi:Fe flux ratio of 8:1. The *in situ* RHEED patterns collected along the ⟨110⟩ azimuthal direction of (001)-oriented $SrTiO_3$ delineating the three regions are superimposed in Fig. 1. Above 460 °C, RHEED streaks associated with $BiFeO_3$ and additional spots are observed. These spots can be indexed to diffraction from (111)-oriented γ-Fe_2O_3, the presence of which was verified by *ex situ* XRD. For these growth parameters, this temperature represents the boundary between regions I and II. Many authors have observed iron oxide inclusions in $BiFeO_3$ films grown by other techniques, e.g., α-Fe_2O_3 by off-axis rf sputtering[21] and γ-Fe_2O_3 by pulsed laser deposition at low oxygen pressures.[22,23] Between 415 and 460 °C, phase-pure films can be grown indicative of region II. At a temperature below 415 °C, additional spots form, which have been indexed by *ex situ* XRD as (001)- and (110)-oriented $Bi_2O_{2.5}$. The occurrence of these spots corresponds to the phase boundary separating regions II and III. A change of the bismuth flux or the oxygen activity results in a shift of the growth window for single-phase $BiFeO_3$, as indicated by the Ellingham boundaries of the adsorption-controlled growth window in Fig. 1. The O_2 overpressures calculated compare well with what is expected given the enhanced activity of O_3 and our directed gas inlet that locally increases the oxygen pressure at the substrate surface.[20]

It has been reported that the single-phase field of $BiFeO_3$ grown by MBE is broad, with single-phase films as much as 8% Bi-deficient being grown.[9] Two films were grown at different points in region II to investigate the growth temperature dependence on composition. One sample was grown in the middle of region II and the second was grown near the phase boundary between regions II and III. For a Bi:Fe flux ratio of 7:1, substrate temperatures of 405 and 375 °C, respectively, corresponded to these points in the Ellingham diagram. The sample grown at $\sim$375 °C had a stoichiometric composition within the 3% measurement accuracy of Rutherford backscattering spectroscopy and displayed a minimum channeling yield (χ_{min}) of 11%. The film grown at 405 °C was Bi-deficient with a 0.95 (±0.03):1.00 Bi:Fe ratio and a χ_{min} of 16%. Our results indicate that stoichiometric single-phase $BiFeO_3$ films may be prepared at the Bi-rich end of region II, i.e., near the boundary with region III.

An XRD scan of the 30 nm thick $BiFeO_3$/(001) $SrTiO_3$ stoichiometric sample is shown in Fig. 2(a). The film is phase-pure $(10\bar{1}\bar{2})$-oriented $BiFeO_3$ (hexagonal indices are used throughout this letter for $BiFeO_3$). Figure 2(b) shows a high-resolution scan of the $10\bar{1}\bar{2}$ peak exhibiting clear thickness fringes indicative of a smooth film with high crystalline quality. A ω rocking curve from the same film is shown in Fig. 2(c). The full width at half maximum (FWHM) of the $BiFeO_3$ film, 29 arc sec (0.008°), is identical to that of the

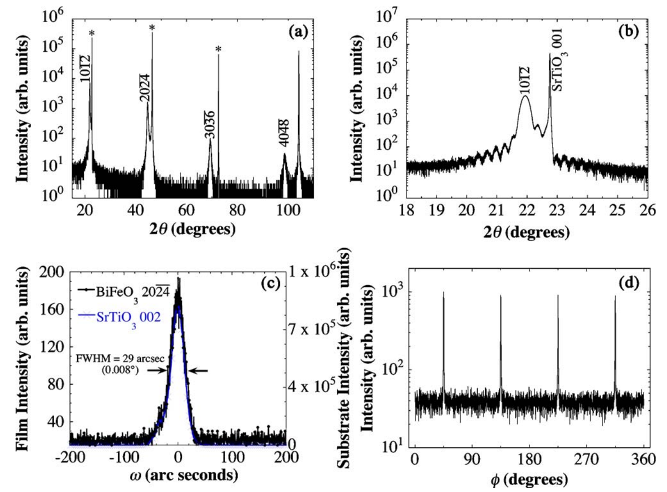

FIG. 2. (Color online) (a) θ-2θ X-ray diffraction pattern of a 30 nm thick $(10\bar{1}\bar{2})$-oriented $BiFeO_3$ film grown on (001) $SrTiO_3$. (b) Shows a close-up of the $10\bar{1}\bar{2}$ peak and thickness fringes. (c) Superimposed ω-rocking curves of the $20\bar{2}\bar{4}$ film and 002 substrate peaks. (d) Azimuthal ϕ scan of $11\bar{2}\bar{3}$ (χ=64.7°) diffraction peaks. χ=90° aligns the diffraction vector to be perpendicular to the plane of the substrate. ϕ=0° corresponds to the projection of the substrate [100] in-plane direction.

underlying substrate indicating that the film crystallinity is substrate limited and is comparable to the narrowest recorded for a $BiFeO_3$ film.[9] Figure 2(d) shows a ϕ scan of the $11\bar{2}\bar{3}$ family of peaks. Four separate peaks are seen, demonstrating that the film is epitaxial with rhombohedral or lower symmetry. Films of cubic or tetragonal symmetry would not exhibit diffraction at these peak positions.[21]

Cross-sectional transmission electron microscopy (TEM) specimens were imaged within a JEOL 3011 high-resolution TEM (HRTEM) that has 0.17 nm point-to-point resolution. Dark-field and HRTEM imaging (not shown) reveals 71° and 109° domain walls, as have been previously observed in films grown by other techniques on nonvicinal (001) $SrTiO_3$ substrates.[24,25] HRTEM verifies the $10\bar{1}\bar{2}$ orientation and reveals an atomically abrupt interface.

As stoichiometry can play a strong role in material properties, we investigated the optical properties and band gaps for the two films grown in different locations within region II. Room temperature ellipsometric spectra (in Δ, ψ) were collected *ex situ* at three angles of incidence, Θ_i=55°, 70°, and 85°, using a variable-angle rotating-compensator multichannel spectroscopic ellipsometer[26,27] over a spectral range from 0.75 to 6.5 eV for the stoichiometric $BiFeO_3$ film and at Θ_i=45°, 60°, and 75° over a spectral range from 0.75 to 5.0 eV for the Bi-deficient film. The dielectric function spectra (ε_1, ε_2) shown in Fig. 3 were extracted using a least squares regression analysis and a weighted root mean square error function[28] to fit the experimental ellipsometric spectra to a four-medium optical model consisting of a semi-infinite $SrTiO_3$ substrate/bulk film/surface roughness/air ambient structure where free parameters correspond to the bulk and surface roughness thicknesses of the $BiFeO_3$ film and a parameterization of the $BiFeO_3$ dielectric function. The dielectric function parameterization of $BiFeO_3$ consists of four Tauc–Lorentz oscillators[29] sharing a common Tauc gap and a constant additive term to ε_1 represented by ε_∞. The optical properties of the surface roughness layer are represented by a Bruggeman

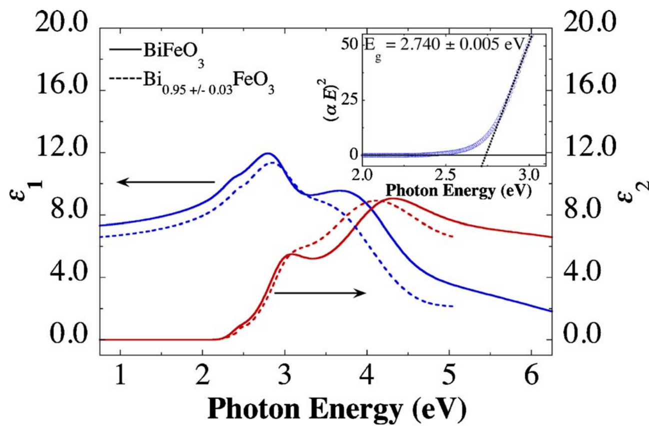

FIG. 3. (Color online) Dielectric function spectra obtained from spectroscopic ellipsometry analysis of stoichiometric (solid lines) and Bi-deficient (dashed lines) 30 nm thick $BiFeO_3$/(001) $SrTiO_3$ over a spectral range from 0.75 to 6.5 eV for the stoichiometric film and from 0.75 to 5.0 eV for the Bi-deficient film.

effective medium approximation[30] consisting of a 50% bulk film/50% void mixture. Although $BiFeO_3$ is rhombohedral and exhibits uniaxial optical anisotropy, these thin films may be treated as isotropic due to their mixed domain structure (i.e., the four twin variants in these films distribute the optic axes along the four ⟨111⟩ pseudocubic $BiFeO_3$ directions within the macroscopic region sampled in the spectroscopic ellipsometry measurement). The experimental real and imaginary dielectric spectra are a combination of the ordinary and extraordinary dielectric functions but, due to the distribution in optical axis orientation, it is impossible to separate the respective contributions.

The onset of optical absorption is observed at 2.07 ± 0.14 eV and 2.11 ± 0.06 eV for the bismuth-deficient and stoichiometric $BiFeO_3$ films, respectively. The direct band gap, obtained from a linear extrapolation of $(\alpha E)^2$ (inset, Fig. 3 for the stoichiometric film) is invariant at 2.74 eV. Band gap measurements on five different MBE-grown $BiFeO_3$ films on (001) $SrTiO_3$, (001) $(LaAlO_3)_{0.3}$-$(SrAl_{0.5}Ta_{0.5}O_3)_{0.7}$ (LSAT), and (111) $SrTiO_3$ (Ref. 31) revealed a direct band gap in all cases with $E_g = 2.77 \pm 0.04$ eV. The invariance of the band gap energy with films of differing strain states suggests that the band gap is relatively insensitive to these effects. This value is consistent with predictions.[32] Previous reports have suggested an indirect gap at lower energies in addition to the direct gap.[5,6] In our data, the lack of the characteristic shape of the $(E\alpha)^{1/2}$ versus energy plot indicating the required phonon participation argues against an indirect gap.[33] It is prudent to consider the optical absorption onset as a joint density of states effect that is very small and likely insignificant in ac conductivity. While the two films studied exhibit stoichiometry differences, the dielectric function spectra show similar absorption onsets and direct band gaps. This is to be expected, as the identical crystal structure and, thus, bonding is present resulting in minute variations in the density of states and band gap. A shift in the resonance energies to lower energy is observed in the dielectric function for the nonstoichiometric film.

This work was supported by the Office of Naval Research through Grant No. N00014-04-1-0426 monitored by Dr. Colin Wood, by NSF through Grant Nos. DMR-0213623 and IIP-0737759, and by the U.S. DOE through Grant Nos. DE-AC02-05CH11231 and DE-FG02-01-ER45885 (UT).

[1]G. A. Smolenskii and I. E. Chupis, Sov. Phys. Usp. **25**, 475 (1982).
[2]J. Wang, J. B. Neaton, H. Zheng, V. Nagarajan, S. B. Ogale, B. Liu, D. Viehland, V. Vaithyanathan, D. G. Schlom, U. V. Waghmare, N. A. Spaldin, K. M. Rabe, M. Wuttig, and R. Ramesh, Science **299**, 1719 (2003).
[3]V. V. Shvartsman, W. Kleemann, R. Haumont, and J. Kreisel, Appl. Phys. Lett. **90**, 172115 (2007).
[4]D. Lebeugle, D. Colson, A. Forget, M. Viret, P. Bonville, J. F. Marucco, and S. Fusil, Phys. Rev. B **76**, 024116 (2007).
[5]V. Fruth, E. Tenea, M. Gartner, A. Anastasescu, D. Berger, R. Ramer, and M. Zaharescu, J. Eur. Ceram. Soc. **27**, 937 (2007).
[6]T. P. Gujar, V. R. Shinde, and C. D. Lokhande, Mater. Chem. Phys. **103**, 142 (2007).
[7]T. Kanai, S. Ohkoshi, and K. Hashimoto, J. Phys. Chem. Solids **64**, 391 (2003).
[8]F. Gao, Y. Yuan, K. F. Wang, X. Y. Chen, F. Chen, and J. M. Liu, Appl. Phys. Lett. **89**, 102506 (2006).
[9]J. F. Ihlefeld, A. Kumar, V. Gopalan, D. G. Schlom, Y. B. Chen, X. Q. Pan, T. Heeg, J. Schubert, X. Ke, P. Schiffer, J. Orenstein, L. W. Martin, Y. H. Chu, and R. Ramesh, Appl. Phys. Lett. **91**, 071922 (2007).
[10]G. Koster, B. L. Kropman, G. Rijnders, D. H. A. Blank, and H. Rogalla, Appl. Phys. Lett. **73**, 2920 (1998).
[11]L. Kaufman, CALPHAD: Comput. Coupling Phase Diagrams Thermochem. **25**, 141 (2001).
[12]R. Heckingbottom, G. J. Davies, and K. A. Prior, Surf. Sci. **132**, 375 (1983).
[13]H. Seki and A. Koukitu, J. Cryst. Growth **78**, 342 (1986).
[14]J. Y. Tsao, J. Cryst. Growth **110**, 595 (1991).
[15]J. Y. Tsao, *Materials Fundamentals of Molecular Beam Epitaxy* (Academic, Boston, 1993).
[16]Z. K. Liu, D. G. Schlom, Q. Li, and X. X. Xi, Appl. Phys. Lett. **78**, 3678 (2001).
[17]D. G. Schlom, J. H. Haeni, J. Lettieri, C. D. Theis, W. Tian, J. C. Jiang, and X. Q. Pan, Mater. Sci. Eng., B **87**, 282 (2001).
[18]Scientific Group Thermodata Europe, *Thermodynamic Properties of Inorganic Materials*, in Landolt-Börnstein New Series, Group IV, Vol. 19, edited by Lehrstuhl für Theoretische Hüttenkunde (Springer, Berlin, 1999).
[19]J. O. Andersson, T. Helander, L. H. Hoglund, P. F. Shi, and B. Sundman, CALPHAD: Comput. Coupling Phase Diagrams Thermochem. **26**, 273 (2002).
[20]D. G. Schlom and J. S. J. Harris, in *Molecular Beam Epitaxy: Applications to Key Materials*, edited by R. F. C. Farrow (Noyes, Park Ridge, NJ, 1995), pp. 505–622.
[21]R. R. Das, D. M. Kim, S. H. Baek, C. B. Eom, F. Zavaliche, S. Y. Yang, R. Ramesh, Y. B. Chen, X. Q. Pan, X. Ke, M. S. Rzchowski, and S. K. Streiffer, Appl. Phys. Lett. **88**, 242904 (2006).
[22]H. Bea, M. Bibes, A. Barthelemy, K. Bouzehouane, E. Jacquet, A. Khodan, J. P. Contour, S. Fusil, F. Wyczisk, A. Forget, D. Lebeugle, D. Colson, and M. Viret, Appl. Phys. Lett. **87**, 072508 (2005).
[23]H. Bea, M. Bibes, S. Fusil, K. Bouzehouane, E. Jacquet, K. Rode, P. Bencok, and A. Barthelemy, Phys. Rev. B **74**, 020101 (2006).
[24]Y. B. Chen, M. B. Katz, X. Q. Pan, R. R. Das, D. M. Kim, S. H. Baek, and C. B. Eom, Appl. Phys. Lett. **90**, 072907 (2007).
[25]F. Zavaliche, P. Shafer, R. Ramesh, M. P. Cruz, R. R. Das, D. M. Kim, and C. B. Eom, Appl. Phys. Lett. **87**, 252902 (2005).
[26]J. Lee, P. I. Rovira, I. An, and R. W. Collins, Rev. Sci. Instrum. **69**, 1800 (1998).
[27]B. D. Johs, J. A. Woollam, C. M. Herzinger, J. N. Hilfiker, R. A. Synowicki, and C. L. Bungay, Proc. SPIE **72**, 29 (1999).
[28]G. E. Jellison, Thin Solid Films **313**, 33 (1998).
[29]G. E. Jellison and F. A. Modine, Appl. Phys. Lett. **69**, 371 (1996).
[30]H. Fujiwara, J. Koh, P. I. Rovira, and R. W. Collins, Phys. Rev. B **61**, 10832 (2000).
[31]A. Kumar, R. C. Rai, N. J. Podraza, S. Denev, M. Ramirez, Y.-H. Chu, L. W. Martin, J. Ihlefeld, T. Heeg, J. Schubert, D. G. Schlom, J. Orenstein, R. Ramesh, R. W. Collins, J. L. Musfeldt, and V. Gopalan, Appl. Phys. Lett. **92**, 121915 (2008).
[32]S. J. Clark and J. Robertson, Appl. Phys. Lett. **90**, 132903 (2007).
[33]J. Bardeen, F. J. Blatt, and L. H. Hall, in *Photoconductivity Conference*, edited by R. G. Breckenridge, B. R. Russell, and E. E. Hahn (Wiley, New York, 1956), pp. 146–154.